ARCHIVIO ISTITUZIONALE
DELLA RICERCA

Alma Mater Studiorum Università di Bologna
Archivio istituzionale della ricerca

Anomalous mass diffusion in a binary mixture and Rayleigh-Bénard instability

This is the final peer-reviewed author's accepted manuscript (postprint) of the following publication:

Published Version:
Barletta, A., Straughan, B. (2024). Anomalous mass diffusion in a binary mixture and Rayleigh-Bénard instability. PHYSICAL REVIEW. E, 110(4), 1-8 [10.1103/PhysRevE.110.045102].

Availability:
This version is available at: https://hdl.handle.net/11585/999398 since: 2024-12-20

Published:

DOI: http://doi.org/10.1103/PhysRevE.110.045102

Terms of use:

Some rights reserved. The terms and conditions for the reuse of this version of the manuscript are specified in the publishing policy. For all terms of use and more information see the publisher's website.

This item was downloaded from IRIS Università di Bologna (https://cris.unibo.it/).
When citing, please refer to the published version.

(Article begins on next page)

13 October 2026

Anomalous mass diffusion in a binary mixture and Rayleigh-Bénard instability

A. Barletta[1], **B. Straughan**[2]

[1]Department of Industrial Engineering, Alma Mater Studiorum Università di Bologna, Viale Risorgimento 2, 40136 Bologna, Italy

[2]Department of Mathematics, University of Durham, Durham, DH1 3LE, U.K.

Abstract

The onset of the Rayleigh-Bénard instability in a horizontal fluid layer is investigated by assuming the fluid as a binary mixture and the concentration buoyancy as the driving force. The focus of this study is on the anomalous diffusion phenomenology emerging when the mean squared displacement of molecules in the diffusive random walk is not proportional to time, as in the usual Fick's diffusion, but it is proportional to a power of time. The power-law model of anomalous diffusion identifies subdiffusion when the power-law index is smaller than unity, while it describes superdiffusion when the power-law index is larger than unity. This study reconsiders the stability analysis of the Rayleigh-Bénard problem by extending the governing equations to include the anomalous diffusion.

Keywords Natural convection; Rayleigh-Bénard problem; Linear stability analysis; Energy method; Mass diffusion

1 Introduction

Anomalous mass diffusion refers to situations where the typical characteristics deviate from classical models based on Fick's law. Scenarios and phenomena associated with anomalous mass diffusion are classified as subdiffusion and superdiffusion. In subdiffusion, solute molecules move slower than predicted by classical diffusion, while in superdiffusion they move faster. A typical cause of superdiffusion is the long-range interactions between molecules leading to occasional Lévy flights. In fact, Lévy walk is a type of random walk where step sizes are drawn from a Lévy distribution, whose main feature is heavy tails in comparison with the typical Gaussian distribution. There is a wide literature documenting the phenomenology and mathematical modelling of the anomalous diffusion. We refer the reader to the excellent reviews by Metzler and Klafter [1] and by Henry, Langlands and Straka [2].

The physical basis of anomalous diffusion relies on the modelling of the molecular random walk process undergone by the solute molecules in a binary mixture. In fact, the relationship

between the mean squared displacement σ_x^2 of the molecules and time t may be sublinear, linear or superlinear, namely

$$\sigma_x^2 = 2Dt^r, \tag{1}$$

where D is the generalised diffusion coefficient (with SI units $\mathrm{m}^2/\mathrm{s}^r$) and r is the anomalous diffusion index. Such an index can be $r < 1$ meaning subdiffusion, $r = 1$ leading to the usual linear model of diffusion or $r > 1$ meaning superdiffusion.

There are experimental studies and measurements of anomalous diffusion in a plethora of cases involving, for instance, polymers, biopolymers, proteins and liquid crystals, leading to the evaluation of the generalised diffusion coefficient and the power-law index. Examples are the papers by Banks and Fradin [3] and by Martin, Jerolmack and Schumer [4]. We report that fluorescence correlation spectroscopy technique has been employed by many authors [5, 6] for the experimental analysis of anomalous diffusion. For example, Tolić-Nørrelykke et al. [7] provided experimental evidence for subdiffusion of granules in the cytoplasm of a living yeast cell with an anomalous diffusion index $r = 0.75$. On the other hand, a superdiffusion behaviour had been observed by Gal and Weihs [8], who reported a value $r = 1.25$ for the case of polymeric particles diffusing into cancer cells.

The classical Rayleigh-Bénard problem has alternative versions where mass diffusion emerges in combination with heat transfer or with the destabilising contribution of one or more concentration gradients. Early investigations of the solutal Rayleigh-Bénard problem were published several decades ago [9, 10]. In recent years, this topic has been revisited by other authors [11–15] pointing out new scenarios such as triple diffusion, viscoelasticity, Soret effect and viscous dissipation. The problem of double diffusion is of immense importance due to many applications, such as to sea ice melting [16], convective motion in volcanic caldera [17, 18], and to renewable energy generation via solar ponds [19].

The aim of this paper is reconsidering the stability analysis of the Rayleigh-Bénard system, under conditions of either subdiffusion or superdiffusion. The analysis is first approached with the linearised set of governing equations for the perturbations and a normal mode analysis. Then, the energy method is employed to approach nonlinearly the case of superdiffusion. The energy method is also employed to reconsider the linear analysis of the instability for the case of subdiffusion under a broader perspective not based on normal modes. This paper extends previous analyses referring to Darcy's flow in a porous medium [20, 21]. We emphasise that our main objective is pointing out the dramatic effects of an even minimal departure from the standard mass diffusion trend of the molecular mean squared displacement variance versus time. We will show that a departure from linearity in this trend may mean a completely different response in terms of stability or instability.

2 The mathematical model

We consider a horizontal fluid layer with thickness H and infinite horizontal width, bounded by two horizontal planes $z = 0$ and $z = H$. The z axis is vertical while the x and y axes are horizontal. The fluid is a binary isothermal mixture. Following the anomalous diffusion

model discussed by Henry, Langlands and Straka [2] and employed in the recent studies by Barletta [20] and by Straughan and Barletta [21], we introduce an effective time-dependent diffusivity, $D\,r\,t^{r-1}$, based on the generalised diffusion coefficient D.

Generally speaking, the biofluids or complex fluids where the phenomenon of anomalous diffusion is displayed may have a non-Newtonian behaviour. However, the Newtonian rheology is a universal limiting case allowed by most non-Newtonian models. The reason is that a Newtonian or non-Newtonian behaviour may arise in relation to the flow regime and to the size of the flow domain. For example, blood flows are studied in the literature according to the Newtonian model as "*blood is modelled as a Newtonian fluid with a constant viscosity of* $\nu = 4.8 \times 10^{-6}\mathrm{m}^2/\mathrm{s}$ *since its non-Newtonian features are relevant only in vessels of sub-millimetric diameter*" [22]. On the other hand, the shear-thinning effect modelled via the Carreau-Yasuda rheology may arise under different conditions. Incidentally, we note that even viscoelastic effects have been pointed out for blood under given unsteady flow conditions [23]. We mentioned blood as a prototypical biofluid, but the arguments raised in the case of blood rheology are mostly valid also for other complex fluids. Furthermore, it should be emphasised that, at small shear rates, every fluid tends to a Newtonian behaviour. This feature does not apply to every non-Newtonian rheological law, but when it does not apply the general understanding, at least for viscous fluids, is that it is a failure of the rheological law. A well-known example is the Ostwald-de Waele model for viscosity, whose singular behaviour at vanishingly small shear rates is considered as an unphysical feature. The universal character of the Newtonian behaviour justifies its interest for a basic characterisation of the onset of instability. The non-Newtonian behaviour is interesting when a specific type of fluids is targeted, which is not the case for our analysis of anomalous diffusion.

By adopting the Newtonian fluid model and the Oberbeck-Boussinesq approximation, we can express the local mass, momentum and solutal concentration balance equations as

$$\begin{aligned}
&\frac{\partial u_j}{\partial x_j} = 0, \\
&\frac{\partial u_i}{\partial t} + u_j\,\frac{\partial u_i}{\partial x_j} = -\beta\,(c - c_0)\,g_i - \frac{1}{\rho_0}\,\frac{\partial p}{\partial x_i} + \nu\,\nabla^2 u_i, \\
&\frac{\partial c}{\partial t} + u_j\,\frac{\partial c}{\partial x_j} = D\,r\,t^{r-1}\,\nabla^2 c.
\end{aligned} \tag{2}$$

Here, Einstein's notation for implicit summation over repeated indexes has been adopted. Furthermore, the fields expressing the velocity, dynamic pressure, and concentration have been denoted as u_i, p and c, respectively. The dynamic pressure is the difference between the pressure and the hydrostatic pressure, while symbol c_0 is the reference concentration employed for the definition of the buoyancy force. Fluid properties β, ρ_0 and ν denote the mass expansion coefficient, the reference density and the kinematic viscosity, respectively. The gravitational acceleration is given by $g_i = -g\,\delta_{i3}$, where g is the modulus of g_i and δ_{i3} is the $i3$ component of Kronecker's delta, namely, the i component of the unit vector along the z axis.

Given that the boundaries $z = 0, H$ are assumed with uniform concentrations c_1 and c_2, respectively, there are different combinations of stress-free and rigid boundary conditions for

the velocity that are usually employed. For the sake of simplicity, we will hereafter assume stress-free boundary conditions at both boundaries, as this is the only case leading to an analytical solution in the standard diffusion case, $r = 1$.

2.1 The basic solution

A stationary basic solution of (2) satisfying the boundary conditions can be found with the velocity, dynamic pressure gradient and solute concentration expressed as

$$u_{bi} = 0, \quad \frac{\partial p_b}{\partial x_i} = -\rho_0 \left(c_b - c_0\right) g_i, \quad c_b = c_1 - \frac{c_1 - c_2}{H} z, \tag{3}$$

where the subscript b stands for basic state. This is exactly the basic state considered in the traditional Rayleigh-Bénard problem with standard diffusion, as the value of r does not influence the solution.

2.2 Perturbing the basic state

We introduce a small-amplitude perturbation of the basic state by defining

$$u_i = u_{bi} + U_i, \quad p = p_b + P, \quad c = c_b + C, \tag{4}$$

where (U_i, P, C) are small perturbation fields. By substituting equations (3) and (4) into (2) and by neglecting the nonlinear terms in the perturbations, we obtain

$$\begin{aligned}
&\frac{\partial U_j}{\partial x_j} = 0, \\
&\frac{\partial U_i}{\partial t} = -\beta\, C\, g_i - \frac{1}{\rho_0}\frac{\partial P}{\partial x_i} + \nu\, \nabla^2 U_i, \\
&\frac{\partial C}{\partial t} - W\, \frac{c_1 - c_2}{H} = D\, r\, t^{r-1}\, \nabla^2 C,
\end{aligned} \tag{5}$$

where W denotes the z component of U_i, while the x and y components will be denoted as U and V. Thus, the boundary conditions can be expressed as

$$z = 0, H: \qquad W = 0 = C, \quad \frac{\partial U}{\partial z} = 0 = \frac{\partial V}{\partial z}. \tag{6}$$

Equations (5) and (6) can be rewritten in a dimensionless form by means of the scaling

$$\frac{U_i}{H/\tau} \to U_i, \quad \frac{C}{c_1 - c_2} \to C, \quad \frac{P}{\rho_0 \nu/\tau} \to P, \quad \frac{x_i}{H} \to x_i, \quad \frac{t}{\tau} \to t, \tag{7}$$

where $\tau = (H^2/D)^{1/r}$ is the diffusion time constant. Thus, equations (5) yield

$$\begin{aligned}
&\frac{\partial U_j}{\partial x_j} = 0, \\
&\left(\frac{1}{\mathrm{Sc}}\,\frac{\partial}{\partial t} - \nabla^2\right) U_i = \mathrm{Ra}\, C\, \delta_{i3} - \frac{\partial P}{\partial x_i}, \\
&\frac{\partial C}{\partial t} - W = r\, t^{r-1} \nabla^2 C,
\end{aligned} \tag{8}$$

with the boundary conditions

$$z = 0, 1: \qquad W = 0 = C, \quad \frac{\partial U}{\partial z} = 0 = \frac{\partial V}{\partial z}. \tag{9}$$

In equations (8), the Schmidt number and the Rayleigh number are defined as

$$\mathrm{Sc} = \frac{\nu}{D\,\tau^{r-1}}, \quad \mathrm{Ra} = \frac{g\beta(c_1 - c_2)H^3}{\nu D\,\tau^{r-1}}. \tag{10}$$

While β and $c_1 - c_2$ can be either positive or negative, the inequality $\mathrm{Ra} > 0$ addresses a case where the basic state features a potentially unstable solutal stratification. By taking the curl of the second equation (8), one can get rid of the dynamic pressure gradient, $\partial P/\partial x_i$, so that (8) can be reformulated in terms only of the fields W and C, namely

$$\begin{aligned}
&\left(\frac{1}{\mathrm{Sc}}\,\frac{\partial}{\partial t} - \nabla^2\right) \nabla^2 W = \mathrm{Ra}\, \hat{\nabla}^2 C, \\
&\frac{\partial C}{\partial t} - W = r\, t^{r-1} \nabla^2 C,
\end{aligned} \tag{11}$$

with boundary conditions

$$z = 0, 1: \qquad W = 0 = C, \quad \frac{\partial^2 W}{\partial z^2} = 0. \tag{12}$$

In (11), the operator $\hat{\nabla}^2$ stands for the two-dimensional Laplacian,

$$\hat{\nabla}^2 = \frac{\partial^2}{\partial x^2} + \frac{\partial^2}{\partial y^2}. \tag{13}$$

3 Normal mode analysis

Let us test the time evolution of normal mode solutions of (11) and (12), namely

$$W = f(t)\, F_k(x, y)\, \sin(n\pi z), \quad C = h(t)\, F_k(x, y)\, \sin(n\pi z), \qquad n = 1, 2, 3, \ \ldots\ , \tag{14}$$

chosen so that the boundary conditions (13) are identically satisfied. In (14), $F_k(x, y)$ is any solution of the two-dimensional Helmholtz equation $\hat{\nabla}^2 F_k(x, y) = -k^2\, F_k(x, y)$, where

k is a real parameter defining the wavenumber of the normal mode [24]. For example, with $F_k(x,y) = \sin(kx)$, (14) describes plane waves propagating in any horizontal direction. In fact, the x axis is chosen arbitrarily as no preferred horizontal direction exists for the system. Substitution of (14) into (11) yields

$$\begin{aligned} &\frac{1}{\mathrm{Sc}}\frac{\mathrm{d}f}{\mathrm{d}t} + a_{n,k}^2\, f - \frac{k^2\mathrm{Ra}}{a_{n,k}^2}\, h = 0, \\ &\frac{\mathrm{d}h}{\mathrm{d}t} - f + r\, t^{r-1} a_{n,k}^2\, h = 0, \end{aligned} \tag{15}$$

where the shorthand notation,

$$a_{n,k}^2 = n^2\pi^2 + k^2, \tag{16}$$

is employed.

3.1 The limit of infinite Schmidt number

There is a simple solution that can be achieved in the limiting case of creeping flow when viscous effects are dominant over diffusion. Such a solution is obtained by taking the limit $\mathrm{Sc} \to \infty$ in (15). In this limiting case, the solution of (15) is expressed as

$$f(t) = a_{n,k}^2\, \sigma\, h(t), \quad h(t) = h(0)\, e^{a_{n,k}^2(\sigma\, t - t^r)}, \tag{17}$$

where σ is a neutral stability parameter defined as

$$\sigma = \frac{k^2\mathrm{Ra}}{a_{n,k}^6}. \tag{18}$$

The behaviour of $f(t)$ and $h(t)$ at large times is firstly determined by r and, if and only if $r = 1$, it is influenced by the neutral stability parameter σ. In fact, equation (17) yields

$$\lim_{t\to+\infty} \begin{pmatrix} f(t) \\ h(t) \end{pmatrix} = \begin{cases} \infty, & \text{for} \quad r < 1, \\ 0, & \text{for} \quad r > 1. \end{cases} \tag{19}$$

For the case of standard diffusion, $r = 1$, both $f(t)$ and $h(t)$ for $t \to +\infty$ tend to 0 if $\sigma < 1$, they are stationary for $\sigma = 1$, while they tend to infinity if $\sigma > 1$. This is the well-known behaviour for the Rayleigh-Bénard instability reported in many books such as Drazin and Reid [24], Straughan [25] and Barletta [26]. Here, the distinctive feature is the extreme sensitivity of the large time behaviour of disturbances to even minimal departures from $r = 1$. Every uncertainty in the determination of r around 1 may turn stability into instability or vice versa. Such a cornerstone feature has been stressed in similar terms for the case of convective instability in a fluid saturated porous medium by Barletta [20]. A schematic outline of the stability/instability with different r and σ is reported in Fig. 1.

It will become clear from the analysis carried out in the forthcoming section 3.2 that the scheme displayed in Fig. 1 applies also to a finite Schmidt number.

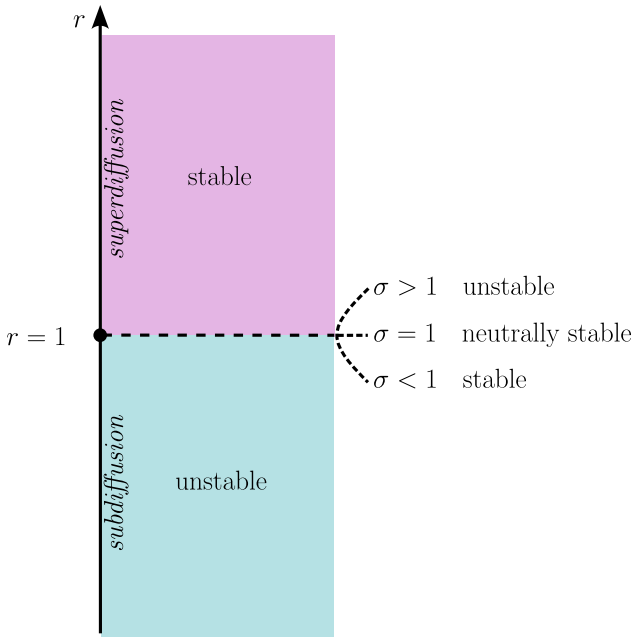

Figure 1: Scheme of the linear instability conditions for different r and σ.

3.2 A finite Schmidt number

The system of first-order differential equations (15) can be rewritten as a single second-order differential equation in the unknown $h(t)$,

$$\frac{\mathrm{d}^2 h}{\mathrm{d}t^2} + a_{n,k}^2\left(\mathrm{Sc} + r\,t^{r-1}\right)\frac{\mathrm{d}h}{\mathrm{d}t} + a_{n,k}^2\left[a_{n,k}^2 r\,\mathrm{Sc}\,t^{r-1} + r(r-1)t^{r-2} - a_{n,k}^2\sigma\,\mathrm{Sc}\right]h = 0. \tag{20}$$

There is just one case where the differential equation (20) has constant coefficients. It is the case of standard diffusion, $r = 1$.

We mention that the test for the instability is based on the large-time behaviour of the solutions of (20). Such an ordinary differential equation is homogeneous, meaning that one may have infinite solutions differing just by an overall constant scale factor. In the following, the challenge we pursue is determining the conditions leading to the existence of solutions of (20) that undergo an unbounded amplification in time when $t \to +\infty$. In fact, this behaviour means instability, while linear stability is found in a parametric range where all possible solutions of (20) are damped in time, with $h(t)$ tending to zero when $t \to +\infty$.

3.2.1 Subdiffusion ($r < 1$)

With subdiffusion, the large-time approximation of (20) is a constant coefficient equation given by

$$\frac{\mathrm{d}^2 h}{\mathrm{d}t^2} + a_{n,k}^2\mathrm{Sc}\,\frac{\mathrm{d}h}{\mathrm{d}t} - a_{n,k}^4\sigma\,\mathrm{Sc}\,h = 0. \tag{21}$$

The general solution of (21) is

$$h(t) = \eta_1 \exp\left[-\frac{a^2 \mathrm{Sc}\, t}{2}\left(\sqrt{\frac{4\sigma}{\mathrm{Sc}}+1}+1\right)\right] + \eta_2 \exp\left[\frac{a^2 \mathrm{Sc}\, t}{2}\left(\sqrt{\frac{4\sigma}{\mathrm{Sc}}+1}-1\right)\right], \tag{22}$$

where η_1 and η_2 are integration constants. If $\sigma > 0$, there are exponentially growing modes at large t. If $\sigma < 0$, one has $\mathrm{Ra} < 0$ and, hence, a stably stratified basic state. In this case, (22) predicts decaying modes at large times either monotonically, if $-\mathrm{Sc}/4 < \sigma < 0$, or oscillatorily, if $\sigma < -\mathrm{Sc}/4$. Thus, our conclusion is that subdiffusion predicts exponentially growing normal modes at large times whenever the basic flow is unstably stratified ($\sigma > 0$ or, equivalently, $\mathrm{Ra} > 0$).

3.2.2 Standard diffusion ($r = 1$)

For the case of standard diffusion, (20) simplifies to

$$\frac{\mathrm{d}^2 h}{\mathrm{d}t^2} + a^2(\mathrm{Sc}+1)\frac{\mathrm{d}h}{\mathrm{d}t} - a^4 \mathrm{Sc}\,(\sigma - 1)\, h = 0, \tag{23}$$

so that the general solution is given by

$$h(t) = \eta_3 \exp\left[-\frac{a^2 t}{2}\left(\mathrm{Sc}+1+\sqrt{\mathrm{Sc}\,(4\sigma+\mathrm{Sc}-2)+1}\right)\right] + \eta_4 \exp\left[-\frac{a^2 t}{2}\left(\mathrm{Sc}+1-\sqrt{\mathrm{Sc}\,(4\sigma+\mathrm{Sc}-2)+1}\right)\right], \tag{24}$$

where η_3 and η_4 are integration constants. From (24), one can conclude that there exist exponentially growing modes whenever $\sigma > 1$. Only monotonically decaying modes are allowed if

$$-\frac{(\mathrm{Sc}-1)^2}{4\mathrm{Sc}} < \sigma < 1. \tag{25}$$

Finally, with a stably stratified basic state ($\sigma < 0$ or, equivalently, $\mathrm{Ra} < 0$), oscillatorily decaying modes are allowed whenever

$$\sigma < -\frac{(\mathrm{Sc}-1)^2}{4\mathrm{Sc}}. \tag{26}$$

These results are in perfect agreement with those obtained for the standard diffusion analysis of the Rayleigh-Bénard instability reported in several books (see, for instance, Drazin and Reid [24] or Chandrasekhar [27]). For the case of thermal diffusion, one has just to replace the Schmidt number with the Prandtl number.

3.2.3 Superdiffusion ($r > 1$)

With superdiffusion, the large-time approximation of (20) is given by

$$\frac{\mathrm{d}^2 h}{\mathrm{d}t^2} + a_{n,k}^2 r\, t^{r-1} \frac{\mathrm{d}h}{\mathrm{d}t} + a_{n,k}^4 r\, \mathrm{Sc}\, t^{r-1} h = 0. \tag{27}$$

Equation (27) is independent of the neutral stability parameter σ and admits only time-decaying solutions at large times. For example, a possible behaviour is $h(t) \sim e^{-a_{n,k}^2 \mathrm{Sc}\, t}$ which can be gathered from (27) by neglecting, at large times, $\mathrm{d}^2h/\mathrm{d}t^2$ with respect to either $t^{r-1}\mathrm{d}h/\mathrm{d}t$ or $t^{r-1}h$.

Some examples of the behaviour of the solutions $h(t)$ of (27) are illustrated in Fig. 2, where the two cases $r = 1.1$ and $r = 1.5$ are considered with different Schmidt numbers in the range $[0.2, 2]$. Also different modes (n, k) are considered in the different frames. The solutions have been obtained by assuming $t > t_0 = 50$, with $h = 1$ and $\mathrm{d}h/\mathrm{d}t = 1$ at $t = t_0$, where the former condition just fixes the gauge for the solutions of the homogeneous differential equation (27). In all cases considered, the fast decay in time of $h(t)$ is quite evident. Such a decay can be either monotonic or oscillatory depending, mainly, on the values of r and Sc. We report that the value assigned to $\mathrm{d}h/\mathrm{d}t$ at $t = t_0$ affects the evolution of $h(t)$ at the earlier stages, while the final decay to zero at later times remains unaltered. We mention that starting the numerical solution at $t = t_0 = 50$ is just a way to address practically the condition of large times underpinning (27).

It is quite important to stress the independence of the time evolution of $h(t)$, at large times, from the neutral stability parameter σ and, hence, from the Rayleigh number Ra. As already pointed out, this is testified by (27). The physical interpretation is that the large time behaviour of the linear disturbances is unaffected by the buoyancy force, so that the ultimate evolution of the normal modes is diffusion dominated. In other words, the extremely efficient diffusion mechanism of superdiffusion is the key reason of the normal mode damping at large times. Thus, superdiffusion leads to linear stability whatever is the value of σ or Ra.

4 Superdiffusion, nonlinear theory, fixed surfaces

The behaviour predicted by the linear theory for the case of subdiffusion is one of perturbations with an initially small amplitude being amplified in time. Such an unstable behaviour cannot be negated by the nonlinear analysis, as finite amplitude perturbations cannot turn out to be stable when infinitesimally small perturbations are unstable. The scenario is evidently different for the case of superdiffusion where the linear theory predicts stability. A stable behaviour displayed by small amplitude perturbations can, at least in principle, be turned into an unstable behaviour by perturbations with a sufficiently large initial amplitude.

We now analyse the fully nonlinear superdiffusion case. The equations are again (8), but

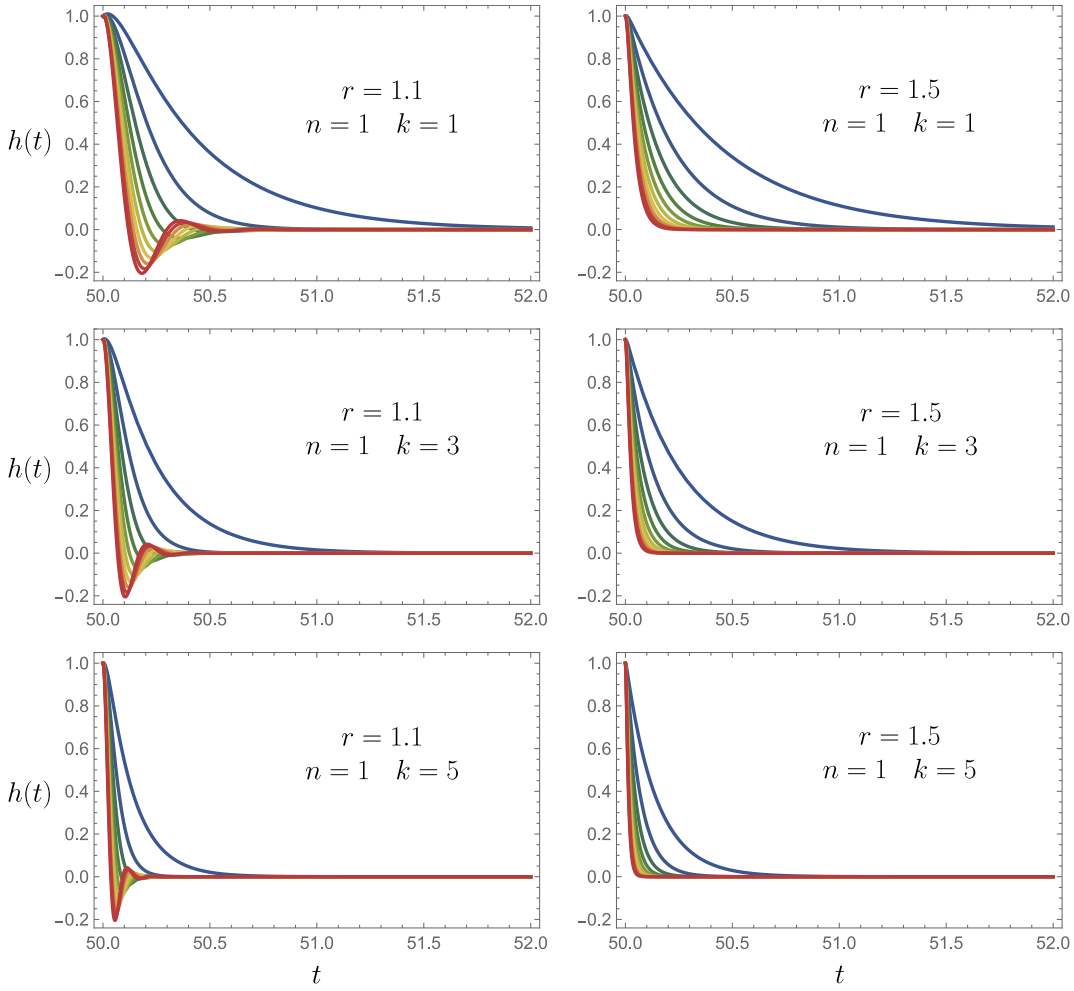

Figure 2: Superdiffusion: plots of the solutions $h(t)$ of (27) with $t > 50$ for different values of Sc ranging from 0.2 (blue) to 2 (red) in steps of 0.2.

we rescale C as $\phi = RC$, where $\mathrm{Ra} = R^2$. Thus, the nonlinear perturbation equations yield

$$\begin{aligned} &\frac{\partial U_j}{\partial x_j} = 0, \\ &\frac{1}{Sc}\Big(\frac{\partial U_i}{\partial t} + U_j\frac{\partial U_i}{\partial x_j}\Big) = \nabla^2 U_i + R\phi\delta_{i3} - \frac{\partial P}{\partial x_i}, \\ &\frac{\partial \phi}{\partial t} + U_i\frac{\partial \phi}{\partial x_i} = RW + rt^{r-1}\nabla^2\phi. \end{aligned} \tag{28}$$

We now consider the case of two fixed surfaces and so the boundary conditions are

$$U_i = 0, \quad \phi = 0, \qquad \text{on } z = 0, 1. \tag{29}$$

In addition to (29) the solution is subject to the requirement that (U_i, ϕ, P) satisfy a plane tiling periodicity; such a condition is explained in depth in Chandrasekhar [27, pages 43–52].

The initial conditions are

$$U_i(\mathbf{x},0) = G_i(\mathbf{x}), \quad \phi(\mathbf{x},0) = \Phi(\mathbf{x}). \tag{30}$$

Let $\mathcal{V}$ denote a period cell for a solution to (28)-(30), and let $\|\cdot\|$ and $(\cdot,\cdot)$ denote the norm and inner product on $L^2(\mathcal{V})$. We wish to analyse the asymptotic behaviour of a solution to (28)-(30) as time $t \to \infty$.

We first require a general bound for $\|\mathbf{U}(t)\|$ and $\|\phi(t)\|$. Thus, suppose $r > 1$, then multiply the second equation (28) by U_i and integrate over $\mathcal{V}$, and likewise multiply the third equation (28) by ϕ and integrate over $\mathcal{V}$. Upon employing the boundary conditions one may show

$$\frac{1}{2}\frac{\mathrm{d}}{\mathrm{d}t}\Big(\frac{1}{\mathrm{Sc}}\|\mathbf{U}\|^2 + \|\phi\|^2\Big) = 2R(\phi, W) - \|\boldsymbol{\nabla}\mathbf{U}\|^2 - rt^{r-1}\|\boldsymbol{\nabla}\phi\|^2, \tag{31}$$

$$\frac{1}{2}\frac{\mathrm{d}}{\mathrm{d}t}\Big(\frac{1}{\mathrm{Sc}}\|\mathbf{U}\|^2 + \|\phi\|^2\Big) \leq 2R(\phi, W) - \|\boldsymbol{\nabla}\mathbf{U}\|^2. \tag{32}$$

Next, use the arithmetic-geometric mean inequality on the (ϕ, W) term in (32) and Poincaré's inequality $\|\boldsymbol{\nabla}\mathbf{U}\|^2 \geq \pi^2\|\mathbf{U}\|^2$ to derive from that inequality

$$\frac{\mathrm{d}}{\mathrm{d}t}\Big(\frac{1}{\mathrm{Sc}}\|\mathbf{U}\|^2 + \|\phi\|^2\Big) \leq \frac{2R^2}{\pi^2}\|\phi\|^2 \leq \frac{2R^2}{\pi^2}\Big(\frac{1}{\mathrm{Sc}}\|\mathbf{U}\|^2 + \|\phi\|^2\Big). \tag{33}$$

One integrates (33) to show that for all $t > 0$,

$$\frac{1}{\mathrm{Sc}}\|\mathbf{U}(t)\|^2 + \|\phi(t)\|^2 \leq \Big(\frac{\|\mathbf{G}\|^2}{\mathrm{Sc}} + \|\Phi\|^2\Big)\exp\Big(\frac{2R^2 t}{\pi^2}\Big). \tag{34}$$

To derive an asymptotic solution estimate we return to equation (31) and then use Poincaré's inequality $\|\boldsymbol{\nabla}\phi\|^2 \geq \pi^2\|\phi\|^2$, and the arithmetic-geometric mean inequality to derive the following inequality:

$$\frac{1}{2}\frac{\mathrm{d}}{\mathrm{d}t}\Big(\frac{1}{\mathrm{Sc}}\|\mathbf{U}\|^2 + \|\phi\|^2\Big) + \frac{\pi^2}{2}\|\mathbf{U}\|^2 + \Big(rt^{r-1}\pi^2 - \frac{2R^2}{\pi^2}\Big)\|\phi\|^2 \leq 0, \tag{35}$$

for all $t > 0$.

We now require $t > t_0 = (2R^2/r\pi^4)^{1/(r-1)}$, and then integrate inequality (35) with respect to time from $2t_0$ to $T > 2t_0$. In this way we find

$$\begin{aligned}
\frac{\pi^2}{2}\int_{2t_0}^{T}\|\mathbf{U}(t)\|^2\,\mathrm{d}t + \int_{2t_0}^{T}\Big(r\pi^2 t^{r-1} - \frac{2R^2}{\pi^2}\Big)\|\phi(t)\|^2\mathrm{d}t \\
&\leq \frac{1}{2\mathrm{Sc}}\|\mathbf{U}(2t_0)\|^2 + \frac{1}{2}\|\phi(2t_0)\|^2 - \frac{1}{2\mathrm{Sc}}\|\mathbf{U}(T)\|^2 - \frac{1}{2}\|\phi(T)\|^2 \\
&\leq \frac{1}{2\mathrm{Sc}}\|\mathbf{U}(2t_0)\|^2 + \frac{1}{2}\|\phi(2t_0)\|^2 \\
&\leq \frac{1}{2\mathrm{Sc}}\Big(\|\mathbf{G}\|^2 + \|\Phi\|^2\Big)\exp\Big[\frac{4R^2 t_0}{\pi^2}\Big] \;\equiv\; K < \infty\,.
\end{aligned} \tag{36}$$

The constant K defined by the expression in (36) is independent of T, and inequality (36) holds for all $T > 2t_0$. The coefficient of the fourth term on the left of (36) satisfies

$$r\pi^2 t^{r-1} - \frac{2R^2}{\pi^2} \geq r\pi^2 (2t_0)^{r-1} - \frac{2R^2}{\pi^2} \equiv \chi > 0.$$

Hence, from (36), one can let $T \to \infty$ to obtain

$$\int_{2t_0}^{\infty} \|\mathbf{U}(t)\|^2 \mathrm{d}t < \frac{2K}{\pi^2}, \quad \text{and} \quad \int_{2t_0}^{\infty} \|\phi(t)\|^2 \mathrm{d}t < \frac{K}{\chi}, \tag{37}$$

so that both integrals are bounded.

Now, we observe from inequality (35) that for $t \geq 2t_0$,

$$\frac{\mathrm{d}}{\mathrm{d}t}\Big(\frac{1}{\mathrm{Sc}}\|\mathbf{U}\|^2 + \|\phi\|^2\Big) \leq 0. \tag{38}$$

Hence, from (37) and (38) we deduce $\|\mathbf{U}(t)\|^2 \to 0$, $\|\phi(t)\|^2 \to 0$, as $t \to \infty$, regardless of the size of the Rayleigh number R^2.

5 Subdiffusion, fixed surfaces

The perturbation equations for subdiffusion are the same as (28), together with the boundary and initial conditions (29), (30). Now, the anomalous diffusion term in (28), $rt^{r-1}\nabla^2\phi$, features $0 < r < 1$.

In this case we deal with the linearised system of equations arising from (28), namely

$$\begin{aligned} &\frac{\partial U_i}{\partial x_i} = 0, \\ &\frac{1}{\mathrm{Sc}}\frac{\partial U_i}{\partial t} = -\frac{\partial P}{\partial x_i} + R\phi\delta_{i3} + \nabla^2 U_i, \\ &\frac{\partial \phi}{\partial t} = RW + rt^{r-1}\nabla^2\phi. \end{aligned} \tag{39}$$

To proceed with an analysis of asymptotic behaviour for a solution to (39), (29), (30), we define the function $F(t)$ by

$$F(t) = \frac{1}{\mathrm{Sc}}\|\mathbf{U}(t)\|^2 + \|\phi(t)\|^2. \tag{40}$$

Differentiate F and use (39), integrate by parts and use the boundary conditions to see that

$$\begin{aligned} \frac{\mathrm{d}F}{\mathrm{d}t} &= \frac{2}{\mathrm{Sc}}\Big(U_i, \frac{\partial U_i}{\partial t}\Big) + 2\Big(\phi, \frac{\partial \phi}{\partial t}\Big), \qquad (41) \\ &= 2\Big(U_i, -\frac{\partial P}{\partial x_i} + R\phi\delta_{i3} + \nabla^2 U_i\Big) + 2\big(\phi, RW + rt^{r-1}\nabla^2\phi\big), \\ &= 4R(\phi, W) - 2\|\boldsymbol{\nabla}\mathbf{U}\|^2 - 2rt^{r-1}\|\boldsymbol{\nabla}\phi\|^2. \qquad (42) \end{aligned}$$

Perform a further differentiation to deduce

$$\begin{aligned}\frac{\mathrm{d}^2F}{\mathrm{d}t^2} &= 4R\left(\frac{\partial\phi}{\partial t}, W\right) + 4R\left(\phi, \frac{\partial W}{\partial t}\right) - 4\left(\frac{\partial U_i}{\partial x_j}, \frac{\partial^2 U_i}{\partial x_j \partial t}\right) - 4rt^{r-1}\left(\frac{\partial\phi}{\partial x_i}, \frac{\partial^2\phi}{\partial x_i \partial t}\right) \\ &\quad - 2r(r-1)t^{r-2}\|\boldsymbol{\nabla}\phi\|^2 \\ &= 4\left(\frac{\partial\phi}{\partial t}, RW + rt^{r-1}\nabla^2\phi\right) + 4\left(\frac{\partial U_i}{\partial t}, R\phi\delta_{i3} + \nabla^2 U_i\right) - 2r(r-1)t^{r-2}\|\boldsymbol{\nabla}\phi\|^2 \\ &= 4\left\|\frac{\partial\phi}{\partial t}\right\|^2 + \frac{4}{\mathrm{Sc}}\left\|\frac{\partial\mathbf{U}}{\partial t}\right\|^2 + 4\left(\frac{\partial U_i}{\partial t}, \frac{\partial P}{\partial x_i}\right) - 2r(r-1)t^{r-2}\|\boldsymbol{\nabla}\phi\|^2 \\ &= 4\left\|\frac{\partial\phi}{\partial t}\right\|^2 + \frac{4}{\mathrm{Sc}}\left\|\frac{\partial\mathbf{U}}{\partial t}\right\|^2 + 2r(1-r)t^{r-2}\|\boldsymbol{\nabla}\phi\|^2 \geq 4\left\|\frac{\partial\phi}{\partial t}\right\|^2 + \frac{4}{\mathrm{Sc}}\left\|\frac{\partial\mathbf{U}}{\partial t}\right\|^2. \end{aligned} \tag{43}$$

Define S^2 by

$$S^2 = \left(\frac{1}{\mathrm{Sc}}\|\mathbf{U}\|^2 + \|\phi\|^2\right)\left(\frac{1}{\mathrm{Sc}}\left\|\frac{\partial\mathbf{U}}{\partial t}\right\|^2 + \left\|\frac{\partial\phi}{\partial t}\right\|^2\right) - \left[\frac{1}{\mathrm{Sc}}\left(U_i, \frac{\partial U_i}{\partial t}\right) + \left(\phi, \frac{\partial\phi}{\partial t}\right)\right]^2, \tag{44}$$

and note that $S^2 \geq 0$ by the Cauchy-Schwarz inequality. Then, employ (40), (41) and (43) to see that

$$F\frac{\mathrm{d}^2F}{\mathrm{d}t^2} - \left(\frac{\mathrm{d}F}{\mathrm{d}t}\right)^2 \geq 0, \tag{45}$$

for all $t > 0$. We assume the initial data are non-zero so that $F^2 > 0$ in some interval beyond $t = 0$. Then, divide (45) by F^2 to see that

$$\frac{\mathrm{d}^2(\log F)}{\mathrm{d}t^2} \geq 0. \tag{46}$$

This inequality is integrated twice and then the exponential is taken of the result to find

$$F(t) \geq F(0)\,\exp\left[\frac{t}{F(0)}\left.\frac{\mathrm{d}F}{\mathrm{d}t}\right|_{t=0}\right]. \tag{47}$$

The form of the right hand side of (47) ensures $F > 0$ for all t. Furthermore, using the initial data and the differential equations

$$\left.\frac{\mathrm{d}F}{\mathrm{d}t}\right|_{t=0} = -2\|\boldsymbol{\nabla}\mathbf{G}\|^2 + 4R(\Phi, G_3). \tag{48}$$

No matter what value R has, there are initial data such that $\mathrm{d}F/\mathrm{d}t|_{t=0} > 0$. Thus, (47) shows that a solution to (39), (29) and (30) in the subdiffusion case will grow exponentially for t large enough.

We have thus demonstrated by rigorous analysis that a solution to the diffusion problem for the Navier-Stokes equations will behave in a similar manner to that found in Section 3

with a normal mode analysis, as well as in Barletta [20] for the analogous problem in a Darcy porous material with no inertia. In the superdiffusion case for the Navier-Stokes equations the solution may grow relatively large for a finite time, but will eventually decay to zero. For the subdiffusion case the solution may also increase or decay for a finite time, but then for the linearised problem the solution will grow at least exponentially as $t \to \infty$.

The predictions of the linear theory at large times and under conditions of instability, where a significant amplification of the initial amplitude of the perturbation occurs, can well be unrealistic. This is a standard situation when the linear analysis of instability is laid out. The treatment presented in this section just yields the energy method approach to the linear dynamics of the perturbations. To the best of authors' knowledge, the energy method does not provide any useful insights into the nonlinear dynamics at large times for the case of subdiffusion. The exploitation of the possible nonlinear saturation effect taking place in the case of subdiffusion, together with the analysis of bifurcations and the evaluation of the mass transfer rates under conditions of cellular flow, deserves a separate analysis to be developed in the future. All this extra information can be gathered by possibly employing the weakly nonlinear stability analysis [24]. However, it must be stressed that even the standard method of the weakly nonlinear analysis has to be reconsidered for anomalous diffusion in order to allow for partial differential equations having time-dependent coefficients.

6 Conclusions

The Rayleigh-Bénard instability in a horizontal binary-mixture fluid layer has been revisited by taking into account the effects devised in the anomalous diffusion model. Such effects are caused by departures from the linear time evolution of the molecular position variance predicted by the standard mass diffusion theory. A power-law time dependence holds instead, leading to either subdiffusion or superdiffusion regimes that occur when the time evolution is sublinear or superlinear, respectively. The mass diffusion equation features a time-dependent diffusion coefficient so that the standard techniques employed for the linear or nonlinear analysis of the Rayleigh-Bénard instability have to be entirely reconsidered. This paper offered one of the first theoretical schemes of how such a stability/instability analysis should be approached. In fact, there exists just a couple of previous investigations sharing the same objective [20, 21]. However, they are relative to the case of Darcy's flow in a porous material.

The modal analysis of the linearised equations for the disturbances has been carried out leading to the formulation of an initial value problem in time to be solved in order to establish the stability/instability of the equilibrium state depending on the subdiffusive, standard or superdiffusive nature of the mass transfer. This analysis has shown that the existence of a neutral stability condition and a critical value of the Rayleigh number Ra is just typical of standard mass diffusion whereas subdiffusion means instability and superdiffusion means stability for every $\mathrm{Ra} > 0$.

The energy method study of the superdiffusion and subdiffusion cases confirmed the results obtained by the modal analysis. In particular, the energy method study of superdiffusion provided an extension of the results obtained through the modal analysis to the

nonlinear case and to the rigid wall version of the velocity boundary conditions.

An evident feature of the anomalous diffusion theory of instability is that it generally rules out the formulation of an eigenvalue problem as the basis for the determination of the instability parametric threshold. On the other hand, the stable/unstable behaviour of the equilibrium state is ascertained by inspecting the large time evolution undergone by the solutions of a differential equation. How this fundamental difference leads to a new systematic scheme for the stability analysis is yet to be investigated and offers a challenge for future research.

Acknowledgements

The work by Antonio Barletta was supported by Alma Mater Studiorum Università di Bologna, grant number RFO-2023. The work of Brian Straughan was supported by the Leverhulme Trust, grant number EM/2019-022/9.

References

[1] R. Metzler, J. Klafter, The random walk's guide to anomalous diffusion: a fractional dynamics approach, Physics Reports 339 (2000) 1–77.

[2] B. I. Henry, T. A. M. Langlands, P. Straka, An introduction to fractional diffusion, in: R. L. Dewar, F. Detering (Eds.), Complex Physical, Biophysical and Econophysical Systems, World Scientific, Singapore, 2010, pp. 37–89.

[3] D. S. Banks, C. Fradin, Anomalous diffusion of proteins due to molecular crowding, Biophysical Journal 89 (2005) 2960–2971.

[4] R. L. Martin, D. J. Jerolmack, R. Schumer, The physical basis for anomalous diffusion in bed load transport, Journal of Geophysical Research: Earth Surface 117 (2012) F01018.

[5] M. Weiss, M. Elsner, F. Kartberg, T. Nilsson, Anomalous subdiffusion is a measure for cytoplasmic crowding in living cells, Biophysical journal 87 (2004) 3518–3524.

[6] J. Vercammen, G. Maertens, Y. Engelborghs, Measuring diffusion in a living cell using fluorescence correlation spectroscopy. A closer look at anomalous diffusion using HIV-1 integrase and its interactions as a probe, in: Fluorescence of Supermolecules, Polymers, and Nanosystems, Springer Series on Fluorescence, Vol. 4, Springer, 2008, pp. 323–338.

[7] I. M. Tolić-Nørrelykke, E.-L. Munteanu, G. Thon, L. Oddershede, K. Berg-Sørensen, Anomalous diffusion in living yeast cells, Physical Review Letters 93 (2004) 078102.

[8] N. Gal, D. Weihs, Experimental evidence of strong anomalous diffusion in living cells, Physical Review E 81 (2010) 020903.

[9] G. Veronis, Effect of a stabilizing gradient of solute on thermal convection, Journal of Fluid Mechanics 34 (1968) 315–336.

[10] P. G. Baines, A. E. Gill, On thermohaline convection with linear gradients, Journal of Fluid Mechanics 37 (1969) 289–306.

[11] K. R. Raghunatha, I. S. Shivakumara, M. S. Swamy, Effect of cross-diffusion on the stability of a triple-diffusive Oldroyd-B fluid layer, Zeitschrift für angewandte Mathematik und Physik 70 (2019) 1–21.

[12] S. H. Saleh, S. A. Haddad, Effect of anisotropic permeability on double-diffusive bidisperse porous medium, Heat Transfer 49 (2020) 1825–1841.

[13] K. R. Raghunatha, I. S. Shivakumara, Triple diffusive convection in a viscoelastic Oldroyd-B fluid layer, Physics of Fluids 33 (2021) 063108.

[14] K. A. Amar, S. C. Hirata, M. N. Ouarzazi, Soret effect on the onset of viscous dissipation thermal instability for Poiseuille flows in binary mixtures, Physics of Fluids 34 (2022) 114101.

[15] K. A. Amar, S. C. Hirata, M. N. Ouarzazi, Weakly nonlinear dynamics of viscous dissipation instability involving Poiseuille flows of binary mixtures, Physics of Fluids 36 (2024) 014102.

[16] M. Carr, A model for convection in the evolution of under-ice melt ponds, Continuum Mechanics and Thermodynamics 15 (2003) 45–54.

[17] C. P. De Campos, D. B. Dingwell, K. T. Fehr, Decoupled convection cells from mixing experiments with alkaline melts from Phlegrean Fields, Chemical Geology 213 (2004) 227–251.

[18] C. P. De Campos, D. B. Dingwell, D. Perugini, L. Civetta, T. K. Fehr, Heterogeneities in magma chambers: Insights from the behavior of major and minor elements during mixing experiments with natural alkaline melts, Chemical Geology 256 (2008) 131–145.

[19] P. Dineshkumar, M. Raja, An experimental study on trapezoidal salt gradient solar pond using magnesium sulfate (MgSO4) salt and coal cinder, Journal of Thermal Analysis and Calorimetry 147 (2022) 10525–10532.

[20] A. Barletta, Rayleigh-Bénard instability in a horizontal porous layer with anomalous diffusion, Physics of Fluids 35 (2023) 104114.

[21] B. Straughan, A. Barletta, Asymptotic behaviour for convection with anomalous diffusion, Continuum Mechanics and Thermodynamics (2024) https://doi.org/10.1007/s00161–024–01291–7.

[22] V. Meschini, F. Viola, R. Verzicco, Heart rate effects on the ventricular hemodynamics and mitral valve kinematics, Computers & Fluids 197 (2020) 104359.

[23] G. B. Thurston, Viscoelasticity of human blood, Biophysical Journal 12 (1972) 1205–1217.

[24] P. G. Drazin, W. H. Reid, Hydrodynamic Stability, Cambridge University Press, 2004.

[25] B. Straughan, The Energy Method, Stability, and Nonlinear Convection, Springer, New York, 2004.

[26] A. Barletta, Routes to Absolute Instability in Porous Media, Springer, New York, 2019.

[27] S. Chandrasekhar, Hydrodynamic and Hydromagnetic Stability, Dover, New York, 1981.